Depletion of TMEM65 leads to oxidative stress, apoptosis, induction of mitochondrial unfolded protein response, and upregulation of mitochondrial protein import receptor TOMM22

Yuto Urushima [1], Misa Haraguchi, Masato Yano [*],[1]

Department of Medical Technology, Faculty of Health Sciences, Kumamoto Health Science University, Kumamoto, 861-5598, Japan

ABSTRACT

Mutation in the transmembrane protein 65 gene (*TMEM65*) results in mitochondrial dysfunction and a severe mitochondrial encephalomyopathy phenotype. However, neither the function of TMEM65 nor the cellular responses to its depletion have been fully elucidated. Hence, we knocked down *TMEM65* in human cultured cells and analyzed the resulting cellular responses. Depletion of TMEM65 led to a mild increase in ROS generation and upregulation of the mRNA levels of oxidative stress suppressors, such as NFE2L2 and SESN3, indicating that TMEM65 knockdown induced an oxidative stress response. A mild induction of apoptosis was also observed upon depletion of TMEM65. Depletion of TMEM65 upregulated protein levels of the mitochondrial chaperone HSPD1 and mitochondrial protease LONP1, indicating that mitochondrial unfolded protein response (UPR^{mt}) was induced in response to TMEM65 depletion. Additionally, we found that the mitochondrial protein import receptor TOMM22 and HSPA9 (mitochondrial Hsp70), were also upregulated in TMEM65-depleted cells. Notably, the depletion of TMEM65 did not lead to upregulation of TOMM22 in an ATF5-dependent manner, although upregulation of LONP1 reportedly occurs in an ATF5-dependent manner. Taken together, our findings suggest that depletion of TMEM65 causes mild oxidative stress and apoptosis, induces UPR^{mt}, and upregulates protein expression of mitochondrial protein import receptor TOMM22 in an ATF5-independent manner.

1. Introduction

The mitochondrion is an organelle that is divided by two membranes, an outer membrane, and an inner membrane. The membranes divide the organelle into four compartments, namely, the outer membrane, intermembrane space, inner membrane, and matrix [1]. Most mitochondrial proteins are coded in the genomic DNA. They are synthesized as precursors in the cytosol and are then imported into the mitochondria [1–3]. Recognition and subsequent translocation of the precursor is mainly performed by the TOM (translocase of the outer membrane) and TIM (translocase of the inner membrane) complexes. The TOM complex contains several proteins including TOMM22 and TOMM40. TOMM22, a receptor of the TOM complex, also acts as an organizer protein that enhances TOM complex formation by the pore forming protein, TOMM40 [4]. Precursors translocated through the TOM and TIM complexes are pulled into matrix by HSPA9 (mitochondrial Hsp70) [1].

Adenosine triphosphate (ATP) generation is an important role of mitochondria. The electron transport chain (ETC) is composed of four complexes (Complex I, II, III, and IV). The ETC coupled with ATP synthase generates ATP, accompanied by the consumption of oxygen in complex IV [5,6]. However, when the function of ETC is disrupted, electrons "leaking" from ETC react with oxygen to generate reactive oxygen species (ROS) [7]. As ROS tend to damage DNA, membrane lipids, and proteins, ROS-detoxification enzymes are induced to protect the cells from damage [7,8]. Additionally, the mitochondrial unfolded protein response (UPR^{mt}) is activated when damaged or misfolded proteins accumulate in mitochondria [9–11]. In UPR^{mt}, some nuclear-encoded mitochondrial chaperones and proteases are synthesized in cytosol and are then imported into mitochondria, in which the chaperones assist in protein folding and the proteases remove the damaged or misfolded proteins [12–14]. In addition, it has been reported that some of the proteins having roles in mitochondrial protein

import, such as TOMM20 (mitochondrial protein import receptor) and TIMM17 (translocase of the inner membrane subunit), are induced by UPR^{mt} [15,16].

A severe loss of mitochondrial proteins causes mitochondrial disease [17]. Leigh syndrome is a severe neurological disorder that is associated with deficiency of respiration complex IV (cytochrome *c* oxidase) [17, 18]. Leigh syndrome French-Canadian (LSFC) variant is a mitochondrial disease in which delay of psychiatric and locomotive development is observed, accompanied by neurodegeneration [18]. LSFC is caused by mutations in the gene encoding leucine-rich pentatricopeptide motif-containing protein (LRPPRC) [19]. LRPPRC is a multifunctional protein involved in regulation of OXPHOS activity, mitophagy, and maturation and export of nuclear mRNA [20]. Recent analysis showed that loss of transmembrane protein 65 (TMEM65) leads to similar deficiency as LSFC [21].

TMEM65 contains three putative transmembrane regions and it is localized in the mitochondrial innermembrane [22]. It has been reported that the loss of TMEM65 induces mitochondrial dysfunction, including decreased oxygen consumption rate, ETC complex IV activity, and citrate synthase activity [21]. However, the molecular function of TMEM65 and cellular response to TMEM65 depletion are yet to be elucidated. The relationship between UPR^{mt} and TMEM65 depletion also remains to be elucidated.

In this study, we aimed to examine TMEM65 depletion-induced cellular responses using TMEM65-targeted siRNA to knock down TMEM65. We specifically studied the effects of TMEM65 depletion on oxidative stress response, apoptosis, proteins involved in UPR^{mt}, and mitochondrial import-related factors.

2. Materials and methods

2.1. Reagents

All reagents were purchased from Sigma-Aldrich (Missouri, USA), Wako (Osaka, Japan), or Takara (Kyoto, Japan) unless otherwise stated.

2.2. Cell culture and transfection

HepG2 cells were cultured in growth medium (Dulbecco's modified Eagle's medium plus 10% fetal calf serum) at 37 °C in a humidified atmosphere containing 5% CO_2. Lipofectamine RNAiMAX (Invitrogen, California, USA) and Opti-MEM I (Gibco, New York, USA) were used to transfect small interfering RNAs (siRNAs). The siRNAs used to knock down TMEM65 mRNA (sense: 5′-CCCAUAUUGAAAUGUCUAUdTdT-3′, antisense: 5′-AUAGACAUUUCAAUAUGGGdTdT-3′), the siRNAs used to knock down ATF5 mRNA (sense: 5′-GCAAGCAAAAGAAGAGAGAdTdT-3′, antisense: 5′-UCUCUCUUCUUUUGCUUGCdTdT-3′), and universal negative control siRNAs (sense: 5′-UUCUCCGAACGUGUCACGUdTdT-

3′, antisense: 5′-ACGUGACACGUUCGGAGAAdTdT-3′) were purchased from JBioS (Saitama, Japan). After siRNA transfection, cells were cultured for 72 h for subsequent analyses.

2.3. Quantitative polymerase chain reaction (qPCR)

Total RNA was isolated from HepG2 cells using TRIzol reagent (Invitrogen, Carlsbad, California, USA). The isolated RNA was reverse transcribed to cDNA using a PrimeScript RT reagent kit (Takara Bio, Osaka, Japan). Using the cDNA as a template, qPCR was performed on LightCycler Nano system (Roche, Basel, Switzerland). The oligonucleotides used for qPCR are listed in Supplementary Table 1. The abundance of the mRNA of the target gene was normalized to that of glyceraldehyde-3-phosphate dehydrogenase (GAPDH) mRNA.

2.4. Immunoblot analysis

HepG2 cells were harvested in ice-cold phosphate-buffered saline (PBS) plus 1 mM ethylene diaminetetraacetic acid (EDTA) and were washed with PBS twice. The cells were lysed using PBS plus 1% Triton X-100, and centrifuged at $10,000 \times g$ for 5 min. The supernatant was recovered and mixed with sodium dodecyl sulfate-polyacrylamide gel electrophoresis (SDS-PAGE) loading buffer. After separation of proteins through SDS-PAGE, the proteins were transferred to polyvinylidene difluoride membranes (PVDF). After blocking with 5% skimmed milk, the membranes were used for immunoblot analysis using enhanced chemiluminescence (ECL) Western Blotting Detection Reagents (GE Healthcare, Buckinghamshire, England), as described previously [23]. Immunoblotting was performed using the following antibodies: anti-TMEM65 antibody (Sigma-Aldrich, Missouri, USA), anti-GAPDH antibody (Novus Biologicals, Colorado, USA), anti-HSPD1 antibody (Sigma-Aldrich, Missouri, USA), anti-LONP1 antibody (Sigma-Aldrich, Missouri, USA), anti-VDAC1 antibody (Calbiochem-Novabiochem, California, USA), and anti-TOMM22 (Tom22) antibody [23]. For detecting protein carbonylation, proteins separated through SDS-PAGE were transferred to PVDF membrane, and treated with 100% methanol. After washing in TBS buffer (50 mM Tris-HCl, pH 7.4, 150 mM NaCl) containing 20% methanol, the membrane was equilibrated in 2 M HCl, followed by treatment with 2,4-dinitrophenylhydrazone (DNPH). After washing with 2 M HCl and followed by equilibration in TBS buffer and blocking with 5% skimmed milk, the membrane was subjected to immunoblot analysis using anti-2,4-dinitrophenyl (DNP) antibody (SHIMA Laboratories, Tokyo, Japan). Chemiluminescence images of membranes were obtained with Ez-Capture MG (ATTO, Tokyo, Japan). Intensity of the detected bands (protein expression levels) was analyzed using ImageJ software (https://imagej.nih.gov/ij/).

2.5. Measurement of ROS generation and apoptosis

HepG2 cells were cultured in microwell plate under conditions mentioned previously. After siRNA transfection, the cells were cultured for 72 h and subsequently used for measurement of ROS generation and apoptosis. To detect ROS generation, cells were treated with CM-H_2DCFDA (Invitrogen) for 30 min and washed three times with Hank's Balanced Salt Solution (HBSS). The intensity of green fluorescence (excitation wavelength, 485 nm; emission wavelength, 535 nm) was measured using Infiniti F200 Pro (TECAN, Zürich, Switzerland). To measure apoptotic cells, HepG2 cells were treated with JC-1 (Dojindo, Kumamoto Japan) for 1 h and washed three times with HBSS. The intensity of green fluorescence (excitation wavelength, 485 nm; emission wavelength, 535 nm) and red fluorescence (excitation wavelength, 535 nm; emission wavelength, 590 nm) was measured using Infiniti F200 Pro.

2.6. Statistical analysis

Data were analyzed using Student's t-test and reported as means ± standard deviation (SD).

3. Results

3.1. Confirmation of TMEM65 depletion

HepG2 cells were transfected with control small interfering RNA (siRNA) and TMEM65-targeted siRNA, and the levels of TMEM65 mRNA and protein were examined (Fig. 1). Both TMEM65 mRNA (Fig. 1A) and protein (Fig. 1B and C) levels were significantly reduced after TMEM65
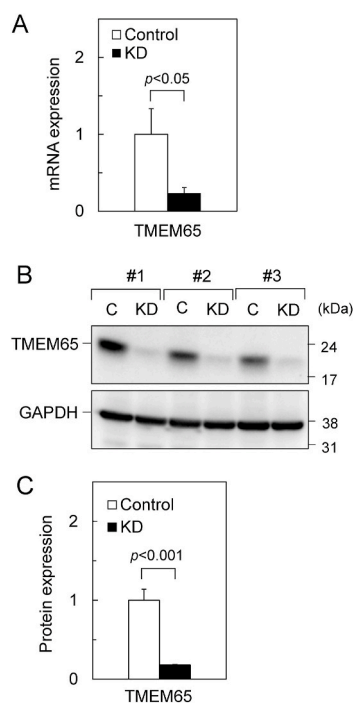
was knocked down using TMEM65-targeted siRNA. Protein levels of GAPDH, a constitutively expressed protein, remained unchanged. These results suggest that TMEM65-targeted siRNA used in this study can specifically knock down TMEM65.

3.2. Depletion of TMEM65 led to mild induction of oxidative stress, apoptosis, and upregulation of ROS-detoxifying genes

To examine the possibility of oxidative stress resulting from TMEM65 depletion-induced mitochondrial dysfunction, mRNA levels of ROS-suppressing genes were measured (Fig. 2A and B). We found that
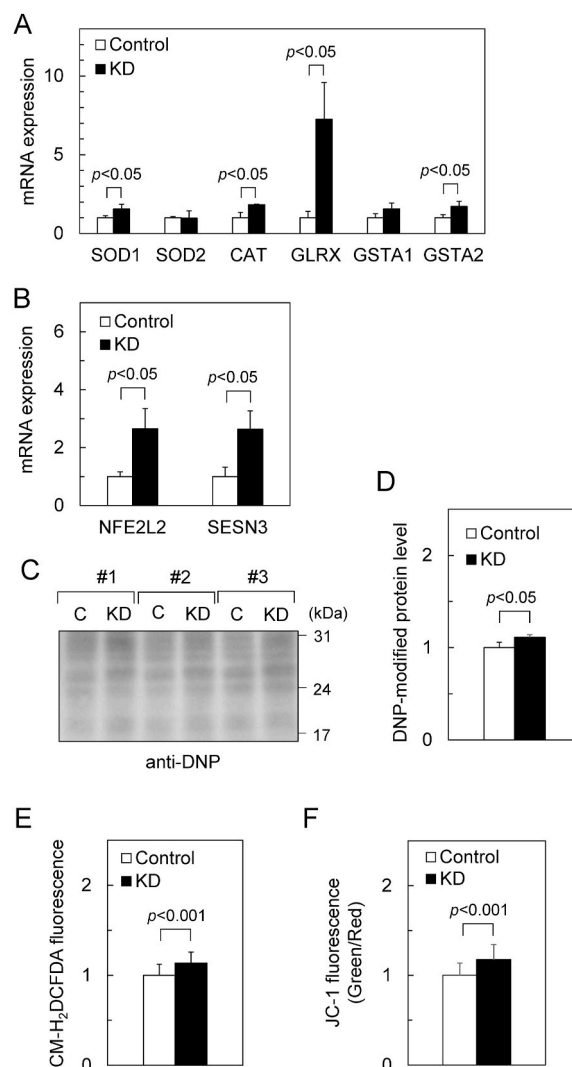

Fig. 2. Depletion of TMEM65 led to induction of oxidative stress, apoptosis, and upregulation of ROS-detoxifying genes. The mRNA levels of ROS-suppressing genes were measured by quantitative PCR (n = 3). The mRNA levels of the controls were considered as 1. (A) SOD1 and SOD2, superoxide dismutase 1 and 2; CAT, catalase; GLRX, glutaredoxin; GSTA1 and GSTA2, glutathione S-transferase alpha 1 and 2; (B) NFE2L2, nuclear factor, erythroid 2 like 2; SESN3, sestrin 3. (C) Carbonylated proteins on the PVDF membrane were detected using DNPH and anti-DNP antibody (see also "Materials and methods") (n = 3). C, control. (D) The DNP-modified protein level was quantified. The levels of DNP-modified protein in the control were set at 1. (E) Fluorescent intensity of CM-H_2DCFDA-loaded cells was measured using Infiniti F200 Pro (n = 48). The levels of CM-H_2DCFDA fluorescence in the control were set at 1. (F) The intensity of both red and green fluorescence of JC-1-loaded cells was measured using Infiniti F200 Pro, and the ratio of green fluorescence to red fluorescence (Green/Red) was calculated (n = 48). The ratio of the fluorescence in the control was set at 1.

Fig. 1. Confirmation of TMEM65 depletion
HepG2 cells were transfected with negative control siRNA (Control) or siRNA for knockdown of TMEM65 (KD), and the cells were cultured for 72 h. (A) Cell extracts were used for measuring mRNA levels of TMEM65 using quantitative PCR (n = 3). The mRNA levels of the control were set as 1. (B) Proteins extracted from cells were subjected to immunoblot analysis to determine TMEM65 protein levels (n = 3). GAPDH, a constitutively expressed protein, was used as the standard. GAPDH, glyceraldehyde-3-phosphate dehydrogenase. C, control. (C) Protein expression of TMEM65 was quantified. The protein expression levels of the control were set at 1.

mRNA levels of the enzymes involved in redox signaling (SOD1, CAT, GLRX, and GSTA2) were significantly increased in the background of TMEM65 depletion (Fig. 2A). In addition, the expression of NFE2L2 (marker of oxidative stress) and SESN3 (repressor of ROS generation) had significantly increased upon TMEM65 depletion (Fig. 2B). These results suggest that TMEM65 depletion resulted in increased ROS generation.

To confirm the increase in ROS generation upon TMEM65 depletion, we next examined whether protein carbonylation induced by ROS was enhanced (Fig. 2C and D). As a result, a small but significant increase in carbonylated protein levels was detected in TMEM65-depleted cells, showing that TMEM65 depletion leads to an increase in ROS generation. To measure ROS generation directly, cells were treated with CM-H_2DCFDA, and the intensity of green fluorescence was measured (Fig. 2E). As a result, a mild but significant increase in CM-H_2DCFDA fluorescence was detected in TMEM65-depleted cells, confirming that depletion of TMEM65 leads to a mild increase in ROS generation.

We further examined whether apoptosis is induced upon TMEM65 depletion. Cells were treated with JC-1, and the intensity of fluorescence in the living cells (red fluorescence) and apoptotic cells (green fluorescence) was measured. As a result, an increase in the ratio of green fluorescence to red fluorescence (Green/Red) was observed (Fig. 2F). This result suggests that apoptosis is mildly induced upon TMEM65 depletion.

3.3. Depletion of TMEM65 led to induction of the expression of UPR^{mt}–related mitochondrial molecular chaperone HSPD1 and protease LONP1

In general, when unfolded and/or misfolded proteins accumulate in mitochondria, UPR^{mt} is activated, and several mitochondrial chaperones and proteases are imported into mitochondria to refold and/or digest those unfolded/misfolded proteins to maintain mitochondrial quality [14]. To examine whether depletion of TMEM65 induced UPR^{mt}, we measured the mRNA levels of mitochondrial molecular chaperone HSPD1 and of proteases, LONP1, CLPP, and YME1L1 (Fig. 3A). As control, mRNA levels of endoplasmic proteins CANX and HSP90B1 were also measured. We found that mRNA levels of HSPD1, LONP1, CLPP, and YME1L1 were significantly elevated when TMEM65 was knocked down, whereas mRNA levels of endoplasmic proteins CANX and HSP90B1 remained unchanged. Increased protein levels of HSPD1 and LONP1 were also observed upon TMEM65 depletion (Fig. 3B and C). Protein expression level of VDAC1, a mitochondrial outer membrane protein, and GAPDH was not changed. These results suggest that depletion of TMEM65 upregulated the expression of UPR^{mt}–related mitochondrial molecular chaperone HSPD1 and protease LONP1.

3.4. Depletion of TMEM65 led to induction of the expression of mitochondrial protein import-related protein TOMM22 in an ATF5-independent manner

We further hypothesized that TMEM65 depletion might lead to upregulation of mitochondrial protein import-related factors to enhance the import of newly synthesized preproteins into mitochondria so that the possible dysfunction of mitochondria lacking TMEM65 could be improved. Therefore, we measured mRNA levels of mitochondrial protein import-related factors (Fig. 4A), and found that TMEM65 depletion significantly increased mRNA levels of TOMM22 and TOMM40 (components of TOM complex), and HSPA9 (mitochondrial Hsp70). Increase in protein levels of TOMM22 and HSPA9 was also observed in TMEM65-knock-down cells (Fig. 4B and C). Protein expression level of VDAC1 and GAPDH was not changed. Thus, depletion of TMEM65 specifically led to upregulation of the expression of mitochondrial protein import-related proteins TOMM22 and HSPA9.

As it has been reported that ATF5 is necessary to induce LONP1 via UPR^{mt} [24], we next examined whether induction of TOMM22 by UPR^{mt}
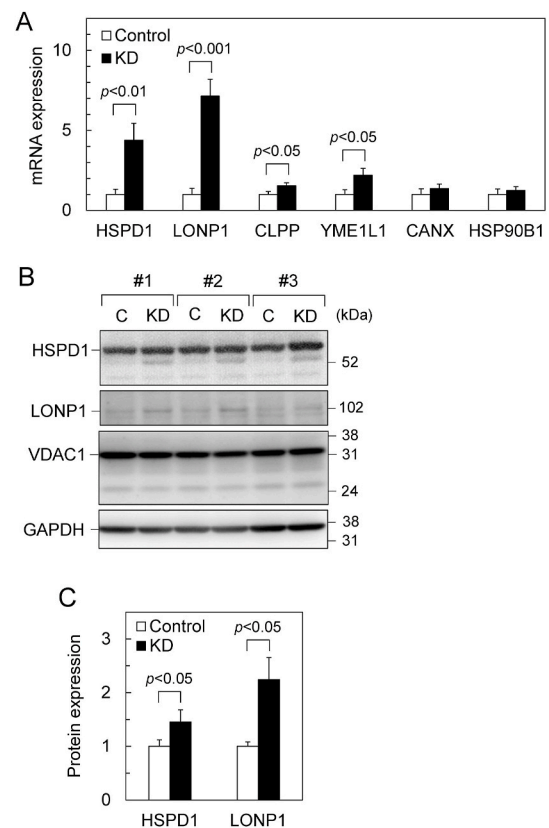

Fig. 3. Depletion of TMEM65 resulted in upregulated expression of UPR^{mt}–related mitochondrial molecular chaperone HSPD1 and protease LONP1. (A) The mRNA levels of the nuclear-encoded proteins typically induced by UPR^{mt} were quantified (n = 3). The genes assessed were mitochondrial heat shock proteins HSPD1 (heat shock protein family D (Hsp60) member 1), mitochondrial protease LONP1 (Lon peptidase 1), YMEL1 (YME1 Like 1 ATPase), and CLPP (caseinolytic mitochondrial matrix peptidase proteolytic subunit). The mRNA levels of the genes encoding endoplasmic proteins CANX (calnexin) and HSP90B1 (heat shock protein 90 beta family member 1) were also measured. The mRNA levels of the control were set at 1. (B) Protein levels of HSPD1, LONP1, VDAC1, and GAPDH were examined by immunoblot analysis (n = 3). C, control. (C) Protein expression of HSPD1 and LONP1 was quantified. The protein expression levels of the control were set at 1.

also requires ATF5 (Fig. 4D). When TMEM65 was depleted, expression of both LONP1 and TOMM22 increased. When both TMEM65 and ATF5 were depleted, upregulation of LONP1 was suppressed, but that of TOMM22 was not suppressed but rather increased. These results suggest that upregulation of TOMM22 by UPR^{mt} does not occur in an ATF5-dependent manner, although upregulation of LONP1 by UPR^{mt} occurs in an ATF5-dependent manner.

4. Discussion

In this study, we examined the cellular responses induced upon TMEM65 depletion, in order to elucidate the role of TMEM65 in mitochondrial function.

We found that oxidative stress response—evidenced by elevated mRNA levels of the enzymes involved in redox signaling (SOD1, CAT, GLRX, GSTA2, NFE2L2, and SESN3)—was evoked in TMEM65-knockdown cells. We also found that protein carbonylation increased upon TMEM65 depletion, confirming increase in ROS generation. However, only slight level of protein carbonylation was observed in TMEM65-knockdown cells. This observation may be attributable to removal of ROS by redox enzymes. Indeed, the direct observation of ROS generation using CM-H_2DCFDA revealed that depletion of TMEM65 led
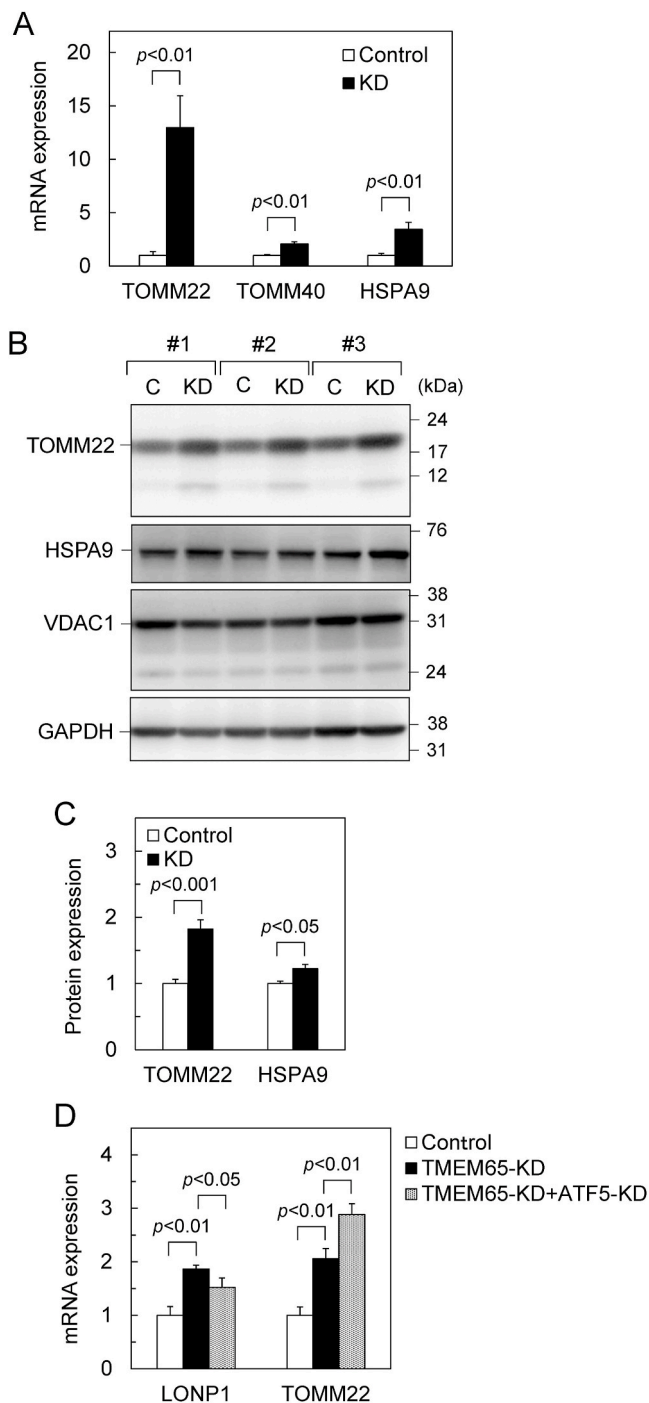
Fig. 4. Depletion of TMEM65 led to induction of the expression of mitochondrial protein import-related proteins TOMM22 in an ATF5-independent manner. (A) The mRNA levels of mitochondrial protein import machinery components were measured (n = 3). The genes assessed were TOMM22, TOMM40, and HSPA9. The mRNA levels of the control were set at 1. TOMM22 and TOMM40, translocase of outer mitochondrial membrane 22 and 40; HSPA9, mitochondrial Hsp70. (B) Protein levels of TOMM22, HSPA9, VDAC1, and GAPDH were examined by immunoblot analysis (n = 3). C, control. (C) Protein expression of TOMM22 and HSPA9 was quantified. The protein expression levels of the control were set at 1. (D) Cells were transfected with negative control siRNA (Control), siRNA for knockdown of TMEM65 (TMEM65-KD), and siRNAs for knockdown of TMEM65 and ATF5 (TMEM65-KD + ATF5-KD). Cell extracts were used for measuring mRNA levels of LONP1 and TOMM22 using quantitative PCR (n = 3). The mRNA levels of the control were set at 1.

to a mild increase in ROS generation. Hence, protein carbonylation induced by ROS may not be a major cause of functional defects in mitochondria in TMEM65-depleted cells. A small induction of apoptosis upon TMEM65 depletion also may not be a major cause of functional defects.

To determine how functional defects occur in TMEM65-depleted mitochondria, we next examined the effects of TMEM65 depletion on UPR^{mt}. We found that mRNA and protein levels of the mitochondrial molecular chaperone HSPD1 and the protease LONP1 had increased in TMEM65-knock-down cells, indicating that UPR^{mt} was induced upon depletion of TMEM65. This observation indicates that TMEM65 depletion results in accumulation of unfolded and/or misfolded proteins and removal of these proteins. The finding seemed to be consistent with a previous report about the reduction of citrate synthase activity following TMEM65 depletion [21].

Furthermore, we found that mRNA and protein levels of the mitochondrial protein import-related proteins (TOMM22 and HSPA9) were elevated in TMEM65-knock-down cells. To date, many proteins have been reported to be induced by UPR^{mt} [25,26]. Some of them are mitochondrial protein import-related proteins [15,16]. However, to our best knowledge, this is the first report to demonstrate that TOMM22 is upregulated by UPR^{mt}. Additionally, we found that upregulation of TOMM22 upon TMEM65 depletion does not occur in an ATF5-dependent manner, suggesting that other transcription factor(s) might be involved in induction of TOMM22 by UPR^{mt}.

Because TOMM22 functions both as an import receptor and as an organizer of the TOM complex containing several proteins including TOMM40 [4], it may be possible that increased levels of TOMM22 will enhance the formation of TOM complex and facilitate preprotein import into the mitochondria. It may be also possible that enhancement of protein import into the mitochondria would partially improve the mitochondrial dysfunction induced by TMEM65 depletion.

5. Conclusions

Although further investigation is necessary to reveal the role played by TMEM65, we have firstly shown in this report that depletion of TMEM65 leads to oxidative stress, apoptosis, induction of UPR^{mt}, and upregulation of mitochondrial protein import receptor TOMM22 in an ATF5-independent manner.

Author statement

I have ensured that the descriptions are accurate and agreed by all authors.

Yuto Urushima performed experiments.

Misa Haraguchi analyzed data.

Masato Yano performed experiments, analyzed data, and wrought this paper.

Declaration of competing interest

The funders had no role in study design, data collection, decision to publish, or preparation of the manuscript. I declare no competing financial interests.

Appendix A. Supplementary data

Supplementary data to this article can be found online at https://doi.org/10.1016/j.bbrep.2020.100870.

References

[1] N. Pfanner, N. Wiedemann, Mitochondrial protein import: two membranes, three translocases, Curr. Opin. Cell Biol. 14 (2002) 400–411. https://www.sciencedirect.com/science/article/abs/pii/S0955067402003551.

[2] A. Chacinska, C.M. Koehler, D. Milenkovic, T. Lithgow, N. Pfanner, Importing mitochondrial proteins: machineries and mechanisms, Cell 138 (2009) 628–644. https://www.sciencedirect.com/science/article/pii/S0092867409009672.

[3] N. Pfanner, B. Warscheid, N. Wiedemann, Mitochondrial proteins: from biogenesis to functional networks, Nat. Rev. Mol. Cell Biol. 20 (2019) 267–284. https://www.nature.com/articles/s41580-018-0092-0.

[4] S. van Wilpe, M.T. Ryan, K. Hill, A.C. Maarse, C. Meisinger, J. Brix, P.J. Dekker, M. Moczko, R. Wagner, M. Meijer, B. Guiard, A. Hönlinger, N. Pfanner, Tom22 is a multifunctional organizer of the mitochondrial preprotein translocase, Nature 401 (1999) 485–489. https://www.nature.com/articles/46802.

[5] F.J. Giordano, Oxygen, oxidative stress, hypoxia, and heart failure, J. Clin. Invest. 115 (2005) 500–508. https://www.ncbi.nlm.nih.gov/pmc/articles/PMC1052012/.

[6] R. Acin-Perez, J.A. Enriquez, The function of the respiratory supercomplexes: the plasticity model, Biochim. Biophys. Acta 1837 (2014) 444–450. https://www.sciencedirect.com/science/article/pii/S0005272813002247.

[7] W.J. Koopman, F. Distelmaier, J.A. Smeitink, P.H. Willems, OXPHOS mutations and neurodegeneration, EMBO J. 32 (2013) 9–29. https://www.ncbi.nlm.nih.gov/pmc/articles/PMC3545297/.

[8] J.W. Zmijewski, A. Landar, N. Watanabe, D.A. Dickinson, N. Noguchi, V.M. Darley-Usmar, Cell signalling by oxidized lipids and the role of reactive oxygen species in the endothelium, Biochem. Soc. Trans. 33 (2005) 1385–1389. https://www.ncbi.nlm.nih.gov/pmc/articles/PMC1413972/.

[9] N.M. Held, R.H. Houtkooper, Mitochondrial quality control pathways as determinants of metabolic health, Bioessays 37 (2015) 867–876. https://onlinelibrary.wiley.com/doi/full/10.1002/bies.201500013.

[10] T. Arnould, S. Michel, P. Renard, Mitochondria retrograde signaling and the UPR^{mt}: where are we in mammals? Int. J. Mol. Sci. 16 (2015) 18224–18251. https://www.ncbi.nlm.nih.gov/pmc/articles/PMC4581242/.

[11] P.M. Quiros, A. Mottis, J. Auwerx, Mitonuclear communication in homeostasis and stress, Nature Rev 17 (2016) 213–226. https://www.nature.com/articles/nrm.2016.23.

[12] J.E. Aldridge, T. Horibe, N.J. Hoogenraad, Discovery of genes activated by the mitochondrial unfolded protein response (mtUPR) and cognate promoter elements, PloS One 2 (2007) e874. https://pubmed.ncbi.nlm.nih.gov/17849004/.

[13] A. Mottis, V. Jovaisaite, J. Auwerx, The mitochondrial unfolded protein response in mammalian physiology, Mamm. Genome 25 (2014) 424–433. https://www.ncbi.nlm.nih.gov/pmc/articles/PMC4167215/.

[14] C. Münch, The different axes of the mammalian mitochondrial unfolded protein response, BMC Biol. 16 (2018) 81. https://www.ncbi.nlm.nih.gov/pmc/articles/PMC6060479/.

[15] A.M. Nargund, C.J. Fiorese, M.W. Pellegrino, P. Deng, C.M. Haynes, Mitochondrial and nuclear accumulation of the transcription factor ATFS-1 promotes OXPHOS recovery during the UPR(mt), Mol. Cell. 58 (2015) 123–133. https://pubmed.ncbi.nlm.nih.gov/25773600/.

[16] Y. Lin, A.M. Schulz, M.W. Pellegrino, Y. Lu, S. Shaham, C.M. Haynes, Maintenance and propagation of a deleterious mitochondrial genome by the mitochondrial UPR, Nature 533 (2016) 416–419. https://pubmed.ncbi.nlm.nih.gov/27135930/.

[17] A.H. Schapira, Mitochondrial disease, Lancet 368 (2006) 70–82. https://www.thelancet.com/journals/lancet/article/PIIS0140-6736(11)61305-6/fulltext.

[18] R.J. Huntsman, D.B. Sinclair, R. Bhargava, A. Chan, Atypical presentations of Leigh syndrome: a case series and review, Pediatr. Neurol. 32 (2005) 334–340. https://www.sciencedirect.com/science/article/abs/pii/S0887899405000342.

[19] V.K. Mootha, P. Lepage, K. Miller, J. Bunkenborg, M. Reich, M. Hjerrild, T. Delmonte, A. Villeneuve, R. Sladek, F. Xu, G.A. Mitchell, C. Morin, M. Mann, T.J. Hudson, B. Robinson, J.D. Rioux, E.S. Lander, Identification of a gene causing human cytochrome c oxidase deficiency by integrative genomics, Proc. Natl. Acad. Sci. U.S.A. 100 (2003) 605–610. https://www.ncbi.nlm.nih.gov/pmc/articles/PMC141043/.

[20] J. Cui, L. Wang, X. Ren, Y. Zhang, H. Zhang, LRPPRC: a multifunctional protein involved in energy metabolism and human disease, Front. Physiol. 10 (2019) 595. https://www.frontiersin.org/articles/10.3389/fphys.2019.00595/full.

[21] A. Nazli, A. Safdar, A. Saleem, M. Akhtar, L.I. Brady, J. Schwartzentruber, M.A. Tarnopolsky, A mutation in the TMEM65 gene results in mitochondrial myopathy with severe neurological manifestations, Eur. J. Hum. Genet. 25 (2017) 744–751. https://www.ncbi.nlm.nih.gov/pubmed/28295037.

[22] N. Nishimura, T. Gotoh, Y. Oike, M. Yano, TMEM65 is a mitochondrial inner-membrane protein, Peer J 2 (2014) e349. https://www.ncbi.nlm.nih.gov/pmc/articles/PMC3994636/.

[23] M. Yano, N. Hoogenraad, K. Terada, M. Mori, Identification and functional analysis of human Tom22 for protein import into mitochondria, Mol. Cell Biol. 20 (2000) 7205–7213. https://www.ncbi.nlm.nih.gov/pmc/articles/PMC86274/.

[24] C.J. Fiorese, A.M. Schulz, Y. Lin, N. Rosin, M.W. Pellegrino, C.M. Haynes, The transcription factor ATF5 mediates a mammalian mitochondrial UPR, Curr. Biol. 26 (2016) 2037–2043. https://pubmed.ncbi.nlm.nih.gov/27426517/.

[25] A. Melber, C. M Haynes, UPR^{mt} regulation and output: a stress response mediated by mitochondrial-nuclear communication, Cell Res. 28 (2018) 281–295. https://pubmed.ncbi.nlm.nih.gov/29424373/.

[26] H.C. Tran, O.V. Aken, Mitochondrial unfolded protein-related responses across kingdoms: similar problems, different regulators, Mitochondrion 53 (2020) 166–177. https://pubmed.ncbi.nlm.nih.gov/32502630/.